A NEW MEMRISTIVE CHAOTIC SYSTEM WITH LARGE-SCALE AMPLITUDE MODULATION AND FIXED-TIME SYNCHRONIZATION

Jian-Ning Huang

School of Mathematics and Information Science
Nanchang Normal University
Nanchang, 330032, China

Qiang Lai

School of Electrical and Automation Engineering
East China Jiaotong University
Nanchang, 330013, China
laiqiang87@126.com

Received 7 February 2026, accepted 6 August 2026, published online 2 September 2026

This paper proposes a new simple memristive chaotic system (MCS) containing an exponential term, a constant term, and a memristor-based nonlinear term. The system has dissipative feature and only one equilibrium. Its parameter-relied complex dynamics are comprehensive studied and the chaos with large parameter regions, multiple bifurcations, and large-scale amplitude modulation are revealed. The proposed system can realize the transition from stability to periodicity via Hopf bifurcation and generate chaos via period-doubling bifurcation with the increase or decrease of multiple parameters. The boundaries of chaotic attractors and the oscillation amplitudes of variables expand over a large-scale range as the parameter values continuously increase, indicating the emergence of large-scale amplitude modulation in the system. Moreover, the fixed-time synchronization (FxTS) problem is studied and the corresponding FxTS conditions are obtained by applying slide mode controller with the designed power reaching law. Both the theoretical derivation and numerical simulation consistently demonstrate the effectiveness of the obtained results.

DOI:10.5506/APhysPolB.57.10-A1

1. Introduction

Chaos theory has experienced rapid development since Lorenz discovered the first butterfly chaotic attractor in 1963 [1]. The chaotic phenomenon have been found in many natural and artificial systems, and their significant influence on the systems' performance have been unlocked, which eradicated the harmful prejudice of chaos and inspired its application exploration in various fields. Scholars have made extensive attempts on chaos research and two mainstream approaches for chaos generation have been formed. One is to chaotify high-dimensional dynamical system or enhance its chaos by using simple feedback control [2]. The other is to modify low-dimensional classic chaotic systems by adding or deleting linear or nonlinear terms to obtain new chaotic systems [3]. Many chaotic systems have been constructed via these two approaches.

A memristor is defined as the fundamental circuit component that represents the relationship between magnetic flux and charge [4]. Accompanied by the discovery and implementation of the memristor [5], memristive chaotic system (MCS) or chaotic system with memristor has sparked a new hot wave of research, especially in recent years, and extensive research progress on MCS has been achieved [6–8]. Zhang *et al.* [9] proposed a 4D conservative MCS by inserting a sine magnetic memristor into the Sprott A system and analyzed its controllable multi-scroll chaos and bursting oscillation. Diao *et al.* [10] used the multi-piecewise memristor to yield MCS with any number of multi-butterfly chaotic attractors. Zhang *et al.* [11] constructed a 4D MCS by introducing a hyperbolic tangent voltage-controlled memristor to the Sprott C system and applied its chaos to design an image encryption algorithm. Njimah *et al.* [12] put forward a new MCS by coupling two Duffing oscillators with a memristor and found its multi-scroll attractors and coexisting oscillations. Chang *et al.* [13] designed a new MCS with extreme multi-stability across multiple parameter regions and revealed its complex dynamics via some numerical experiments. Xu and Ye [14] constructed a four-dimensional (4D) multistable MCS by integrating a three-terminal memtransistor model with a memristor. Zhang and Liu [15] studied the rich dynamical behaviors of MCS with a third-order voltage-controlled generalized memristor. Shi *et al.* [16] proposed two MCSs with a newly designed memristor model, and numerically analyzed the dynamical complexity . By using the discrete-time memristor models, some discrete memristive chaotic maps with hyperchaos and multistability were proposed [17, 18]. A memristor can be used to simulate neural synapse and electromagnetic radiation owing to its unique characteristics, thereby some memristive chaotic neurons and neural networks were proposed. Rajagopal *et al.* [20] constructed a memristive chaotic Chialvo neuron map [19] by incorporating a locally active memristor into the classic Chialvo neuron model. Randrianantenaina *et al.* [21] established a simple memristive chaotic neural network with multi-scroll attractors and offset boosting features. Ryashko and Bashkirtseva [22] studied the combined effect of magnetic induction and random disturbances in the excitation process of a memristive Rulkov neuron and revealed its noise-induced bursting, coherence resonance, and chaotic dynamics, which helps to further understand the role of memristors in enhancing the dynamics of neurons and even chaotic systems. Wang *et al.* [23] established a new memristive chaotic circuit using a memristor emulator, and studied its finite-time synchronization (FTS) with application to image encryption. Lu and Feng [24] investigated the FxTS of a 4D memristive hyperchaotic system by using the slide mode control method. Luo *et al.* [25] applied a simplified controller to realize the synchronization of MCS and basically designed an image encryption scheme with DNA encoding. According to the existing literature, research on MCSs has received widespread attention from scholars and significant progress has been made.

As an important research topic with recent interest, MCS is worth continuing to delve deeper investigation for revealing its unknown dynamical properties and synchronization mechanisms for potential applications. Therefore, this paper aims to establish a new simple one-equilibrium MCS with an exponential nonlinearity and a constant term. The most distinguishing feature of the MCS is that it has large chaotic regions and large-scale amplitude modulation which can flexibly adjust the chaotic signals. The FxTS conditions of the proposed MCS are established through strictly theoretical analysis.

The paper is organized as follows. Section 2 presents the mathematical model of the new MCS. Section 3 numerically illustrates its complex dynamical behaviors. Section 4 theoretically investigate the FxTS with the establishment of sufficient conditions. Section 5 summarizes the conclusions of the whole paper.

2. Model description

Consider a six-term chaotic flow with exponential nonlinearity where the relationships between its state variables can be expressed by [26]

$$\begin{cases} \dot{x} = a(y - x) \\ \dot{y} = xz + e^{z} \\ \dot{z} = k - x \end{cases} . \tag{1}$$

It is a dissipative system with only one equilibrium and simple chaotic behavior for the parameters $a = 8$, $k = 20$. To further enhance the dynamics of system (1), we embed the commonly used memristor model $i = M(w)y$, $\dot{w} = y - w$, where i is the current, y is the voltage, w is the internal state variable, and the memductance is given by $M(w) = p_1 + p_2 |w|$ with $p_1 = 1$ and $p_2 = 0.1$, into system (1) as a feedback term. Taking the internal state of memristor as an additional state, then a new 4D MCS is established and can be written as follows:

$$\begin{cases} \dot{x} = a(y-x) + bM(w)y \\ \dot{y} = cxz + de^{z} \\ \dot{z} = k - x \\ \dot{w} = y - w \end{cases}, \tag{2}$$

where a, b, c, d, k are positive real numbers. Obviously, system (2) is generated on the basis of preserving the basic structure of system (1), and the key is that the introduction of a memristor will greatly enhance and enrich its dynamical behaviors.

Assume $\dot{x} = \dot{y} = \dot{z} = \dot{w} = 0$, then we can get the equilibrium set of system (2) written as

$$O = \{(\bar{x}, \bar{y}, \bar{z}, \bar{w}) | \bar{x} = k, \bar{y} = \bar{w}, ck\bar{z} + de^{\bar{z}} = 0, b\bar{w}|\bar{w}| + 10(a+b)\bar{w} - 10ak = 0\}. \tag{3}$$

Since $c > 0$, $d > 0$, $k > 0$, then the equation $ck\bar{z} + de^{\bar{z}} = 0$ has only one root. As the equation $b\bar{w}\,|\bar{w}| + 10(a+b)\bar{w} - 10ak = 0$ has only one root for $a > 0$, $b > 0$, $k > 0$, then we can confirm that system (2) has only one equilibrium. Linearizing system (2) at the equilibrium and setting $|\lambda I - J| = 0$ (J is the corresponding Jacobian matrix), we can obtain the following characteristic equation that determines the stability of the equilibrium

$$\lambda^4 + r_1\lambda^3 + r_2\lambda^2 + r_3\lambda + r_4 = 0, \tag{4}$$

where $r_1 = 1 + a$, $r_2 = a - ac\bar{z} - bc\bar{z}M(\bar{w})$, $r_3 = (a + bM(\bar{w}))(ck - c\bar{z} + de^{\bar{z}}) - 0.1bcz\,|\bar{w}|$, and $r_4 = (a + b + 0.2\,|\bar{w}|)(ck + de^{\bar{z}})$. Thus, the equilibrium of system (2) is stable if and only if $r_i > 0 (i = 1, 2, 3, 4)$ and $r_1r_2 > r_3, r_1r_2r_3 > r_3^2 + r_4r_1^2$ are satisfied in line with the Routh–Hurwitz stable theory, as all the eigenvalues have negative real parts. Setting $a = 6, b = c = d = 1, k = 9$, we can compute that system (2) has one unstable equilibrium $O(9, 7.0119, -0.1005, 7.0119)$, and a chaotic attractor centered on the equilibrium O is detected by plotting its 2D and 3D projections of phase diagrams, as shown in Fig. 1.

3. Dynamical analysis

To fully understand system (2) and explore its intrinsic dynamics evolved with the parameters, we will give a comprehensive investigation of system (2) via some effective simulation means. System (2) can display rich parameter-relied dynamics including robust chaos, bifurcations, and large-scale amplitude modulation.

Fix the parameters $a = 6$, $b = c = d = 1$ and the initial value (1,1,1,1), then draw the bifurcation diagrams (BDs) and Lyapunov exponents (LEs) to follow the dynamics of system (2) evolved with $k \in [0.1, 100]$, as shown

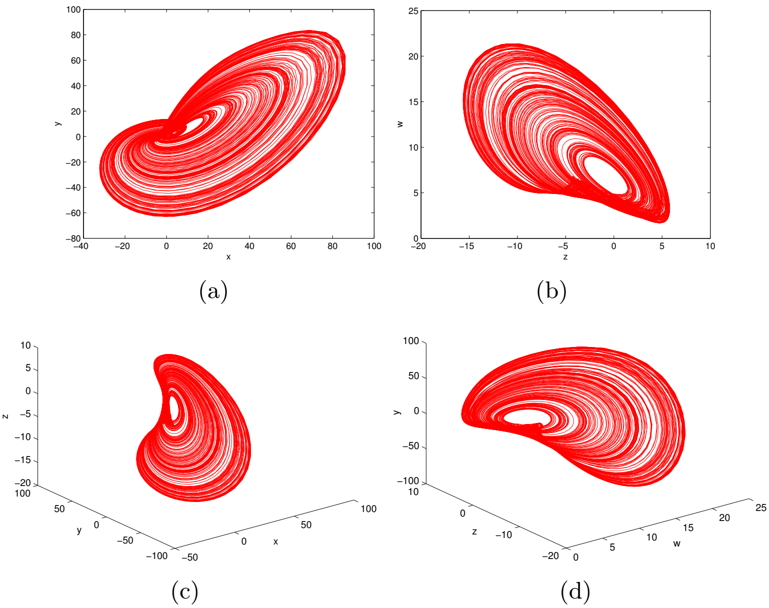

Fig. 1. Chaos of system (2) with parameters $a = 6, b = c = d = 1, k = 9$: (a) $x - y$; (b) $z - w$; (c) $x - y - z$; (d) $w - z - y$.

in Fig. 2. From Fig. 2 (a)–(b), we can easily get that system (2) sequentially experiences stable, periodic, and chaotic states with the increase of k. For $k = 1$, we can compute that system (2) has only one stable equilibrium, $S(1, 0.8469, -0.5671, 0.8469)$, whose eigenvalues $\lambda_1 = -0.9999$, $\lambda_2 = -5.0668$, $\lambda_{3,4} = -0.4666 \pm 1.4560i$ all have negative real parts, and it forms a point attractor as shown in Fig. 3 (a). When k increases across the critical value 1.5740, system (2) losses its stability with the occurrence of Hopf bifurcation and then appears periodic oscillation, which can be seen in Fig. 3 (b) for $k = 2$. Soon afterwards, system (2) enters a chaotic state via a period-doubling bifurcation, as evidenced by the periodic-2, periodic-4, and chaotic attractors for $k = 5, 7.4, 9$, and 18, shown in Fig. 3 (c)–(f). From Fig. 2 (c)–(d), it is clear that system (2) is almost completely in a chaotic state for $k \in [20, 100]$ and the maximum LE increases accordingly, implying that its chaotic behavior is progressively enhanced as the parameter k continues to increase. What is even more interesting is that the boundaries of chaotic attractors widen continuously and the amplitudes of all the state variables x, y, z, w undergo large-scale expansion as the parameter k increases. It can be visually observed from the phase portraits of system (2) for specific parameter values $k = 20, 35, 50$, and 70 in Fig. 4, indicating the emergence of large-scale chaotic amplitude modulation in system (2).

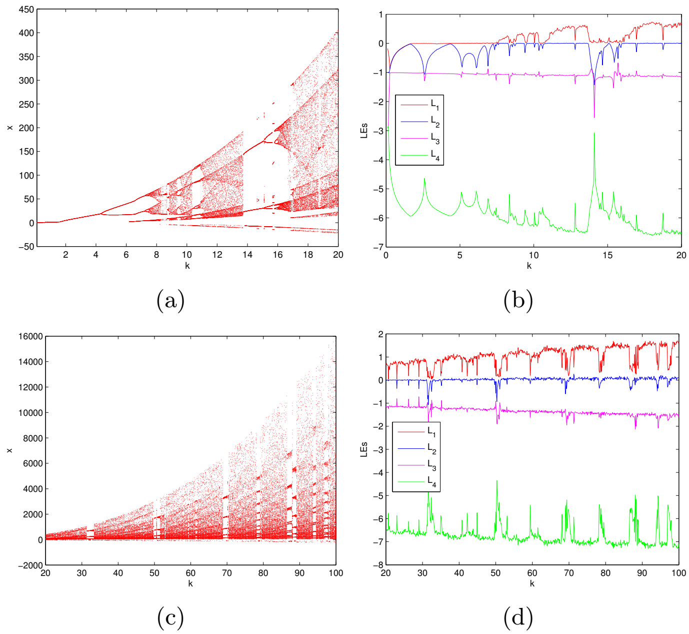

Fig. 2. BDs and LEs of system (2) with parameters $a = 6, b = c = d = 1$: (a) BDs for $k \in [0.1, 20]$; (b) LEs for $k \in [0.1, 20]$; (c) BDs for $k \in [20, 100]$; (d) LEs for $k \in [20, 100]$.

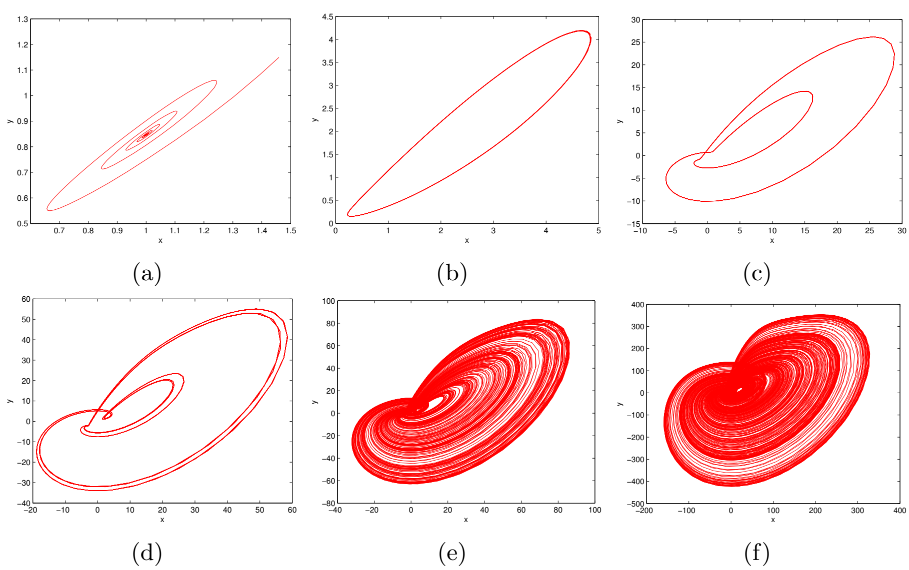

Fig. 3. Attractors of system (2) with different values of k: (a) $k = 1$; (b) $k = 2$; (c) $k = 5$; (d) $k = 7.4$; (e) $k = 9$; (f) $k = 18$.

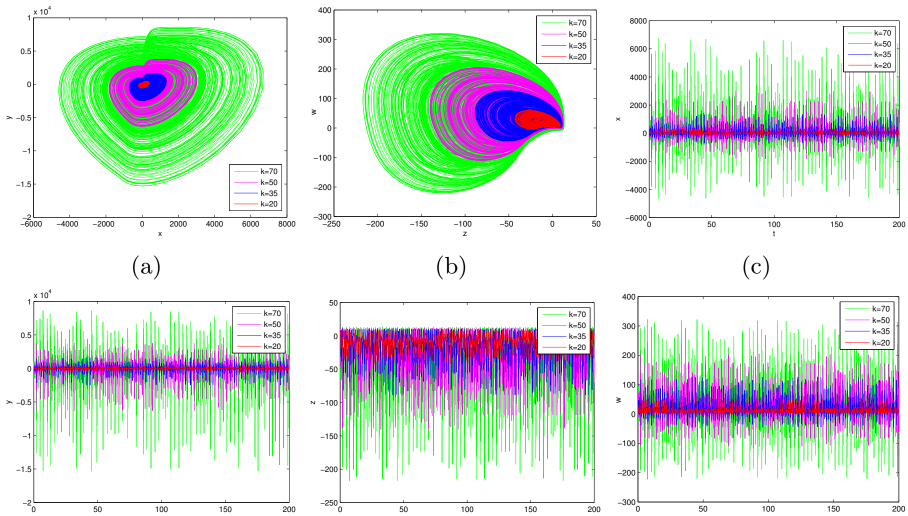

(a) (b) (c)

(d) (e) (f)

Fig. 4. Amplitude modulation of system (2) with different values of k: (a) $x-y$; (b) $z-w$; (c) time series of x; (d) time series of y; (e) time series of z; (f) time series of w.

Fixing the parameters $k=9$, $b=c=d=1$ (or $a=6$, $k=9$, $b=c=1$), we can illustrate the dynamical evolution with respect to $a \in [5,10]$ (or $d \in [5,35]$) by using BDs, as shown in Fig. 5, which implies that system (2) transitions from chaos to a periodic state via an inverse period-doubling bifurcation as the value of a (or d) increases. The chaotic and periodic states can be observed by selecting $a=6,8,10$ (or $d=10,17,20$), as shown in Fig. 6.

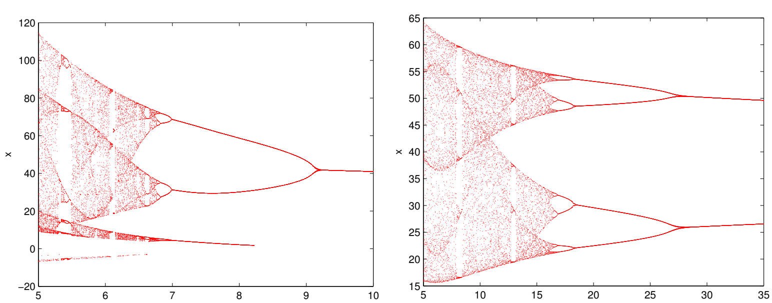

(a) (b)

Fig. 5. BDs of system (2) with the parameters: (a) $a \in [5,10]$, $k=9$, $b=c=d=1$; (b) $d \in [5,35]$, $a=6$, $k=9$, $b=c=1$.

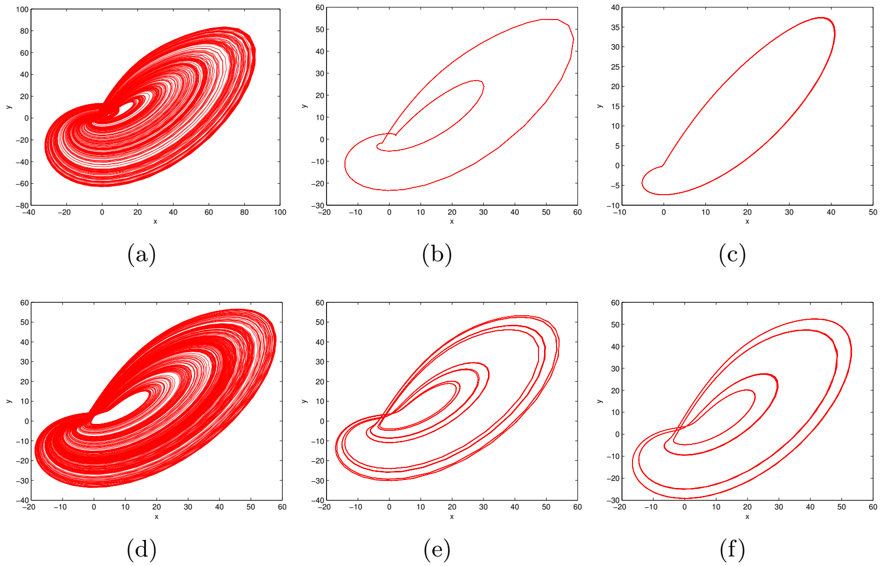

Fig. 6. Attractors of system (2) for an inverse period-doubling bifurcation: (a) chaotic with $a = 6$; (b) periodic-2 with $a = 8$; (c) periodic-1 with $a = 10$; (d) chaotic with $d = 10$; (e) periodic-8 with $d = 17$; (f) periodic-4 with $d = 20$.

System (2) also exhibits an amplitude modulation phenomenon dependent on the parameters b and c that can be similarly illustrated using BDs, LEs, and phase portraits as well. For $a = 6$, $k = 9$, $c = d = 1$ (or $a = 6$, $k = 9$, $b = d = 1$), the BDs and LEs *versus* $b \in [1, 50]$ (or $c \in [1, 10]$) are given in Fig. 7, which shows that system (2) is mostly in a chaotic state and exhibits chaotic amplitude modulation as the values of parameters b and c increase. The phase portraits of chaotic attractors with augmented boundaries are shown in Fig. 8 for $b = 1, 10, 30, 50$ and $c = 4, 5, 7$, and 9, intuitively indicating that the oscillation amplitudea of chaotic state variables are expended by increasing the b and c.

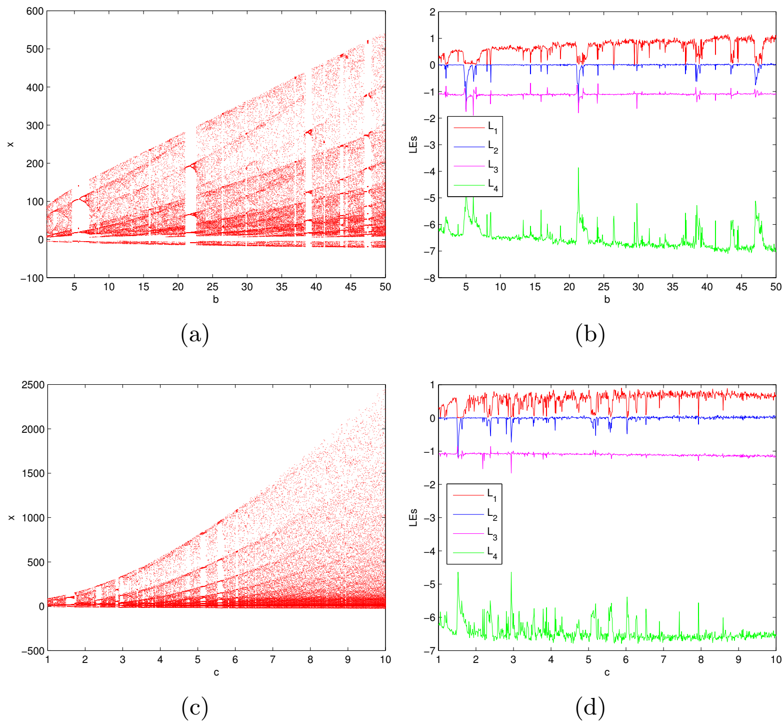

Fig. 7. BDs and LEs of system (2) with the parameters: (a) BDs for $b \in [1, 50]$; (b) LEs for $b \in [1, 50]$; (c) BDs for $c \in [1, 10]$; (d) LEs for $c \in [1, 10]$.

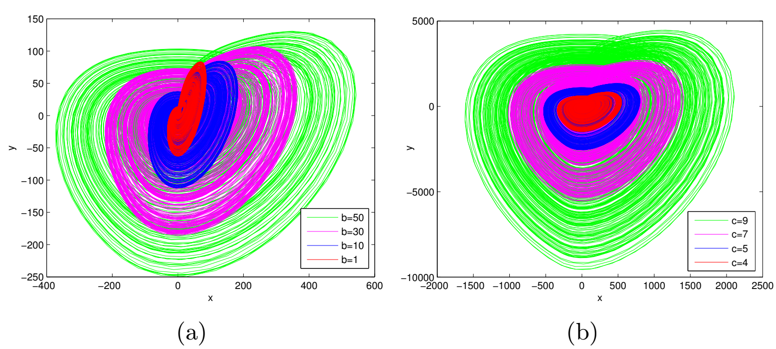

Fig. 8. Amplitude modulation of system (2) for b and c: (a) $b = 1, 10, 30$, and 50; (b) $c = 4, 5, 7$, and 9.

4. Fixed-time synchronization

This section discusses the FxTS problem of system (2) by applying the slide mode control theory and obtains the corresponding sufficient condition for FxTS with theoretical and simulation verifications. Here, we take system (2) as the drive system, and the response system, which has the same equation expression as system (2), is written as follows:

$$\begin{cases} \dot{x}_1 = a(y_1 - x_1) + bM(w_1)y_1 + u_1 \\ \dot{y}_1 = cx_1z_1 + de^{z_1} + u_2 \\ \dot{z}_1 = k - x_1 + u_3 \\ \dot{w}_1 = y_1 - w_1 + u_4 \end{cases} \tag{5}$$

with the control input $u = (u_1, u_2, u_3, u_4)^T$ to be designed. Define the errors of the state variables between drive system (2) and response system (5) as $e_1 = x_1 - x$, $e_2 = y_1 - y$, $e_3 = z_1 - z$, and $e_4 = w_1 - w$. Then we can obtain the error system as follows:

$$\begin{cases} \dot{e}_1 = a(e_2 - e_1) + b[M(w_1)y_1 - M(w)y] + u_1 \\ \dot{e}_2 = c(x_1z_1 - xz) + d(e^{z_1} - e^{z}) + u_2 \\ \dot{e}_3 = -e_1 + u_3 \\ \dot{e}_4 = e_2 - e_4 + u_4 \end{cases} . \tag{6}$$

Thus the FxTS problem between system (2) and system (5) is converted into the fixed-time stability problem of the error system (6). To solve this problem, we use the slide mode control method with numerous advantages. The following definitions and lemmas are given to facilitate the control design and theoretical derivation.

Definition 1 *If there exists a constant $T > 0$ such that $\lim\limits_{t\to T} |e_i(t)| = 0$ and $|e_i(t)| \equiv 0$ $(i = 1, 2, 3, 4)$ for $t \geq T$, then we can say that system (2) and system (5) achieve FTS.*

Definition 2 *If system (2) and (5) synchronize in finite time and the settling time $T_{e(0)}$ is bounded by a positive constant $T_{\max}$ without any relationship with the initial values $e(0)$, that is $T(e(0)) < T_{\max}$, then we can say that system (2) and system (5) achieve FxTS.*

Lemma 1 *For real numbers $\tau_1, \tau_2, \cdots, \tau_n$ and constant $0 < \mu < 1$, the following inequality holds*

$$\left(\sum_{j=1}^{n} |\tau_j|^2\right)^{\frac{\mu+1}{2}} \leq \sum_{j=1}^{n} |\tau_j|^{\mu+1}. \tag{7}$$

Lemma 2 *Assume that there exists a positive definite function $V(t)$ such that*

$$\dot{V}(t) \leq -mV^{\delta}(t) - \gamma V^{\varepsilon}(t)\,, \tag{8}$$

where $m > 0$, $\gamma > 0$, $0 < \delta < 1$, $\varepsilon > 1$, and $V(t) \equiv 0$ for $t \geq T$, then we have

$$T \leq \frac{1}{m(1-\delta)} + \frac{1}{\gamma(\varepsilon - 1)}\,. \tag{9}$$

Here, we will introduce a power reaching law in the slide mode control design to balance the convergence speed and smoothness as follows:

$$\dot{s} = -\gamma_1 s - k_1\,\mathrm{sgn}(s)|s|^{\alpha} - k_2\,\mathrm{sgn}(s)|s|^{\beta} - k_3\,\mathrm{sgn}(s)\,, \tag{10}$$

where k_1, k_2, $k_3 > 0$ are the control parameters, $\gamma_1 > 0$ is the gain of the linear attenuation term, and $0 < \alpha < 1 < \beta$ are the power indices for adjusting the dynamical characteristics of the system. The last term consist of a sign function that can ensure fixed-time convergence of the system under arbitrary initial values. Based on the proposed reaching law (10) and the slide mode reaching condition $s\dot{s} < 0$, we have

$$\dot{V} = s\dot{s} = -\gamma_1 s^2 - k_1|s|^{1+\alpha} - k_2|s|^{1+\beta} - k_3|s| < 0\,. \tag{11}$$

It indicates that the slide surface $s = 0$ is reachable in finite time. For $|s| \gg 1$, $|s|^{\beta} \gg |s|^{\alpha}$. The influence of the lower-order terms in Eq. (10) can be neglected, and $-k_2\,\mathrm{sgn}(s)|s|^{\beta}$ dominates Eq. (10). Then it can be rewritten as

$$\dot{s} \approx -k_2\,\mathrm{sgn}(s)|s|^{\beta}\,. \tag{12}$$

For $|s| \ll 1$, $|s|^{\alpha} \gg |s|^{\beta}$. The influence of the higher-order terms can be neglected in Eq. (10), and $-k_1\,\mathrm{sgn}(s)|s|^{\alpha}$ dominates Eq. (10). Then it can be rewritten as

$$\dot{s} \approx -k_1\,\mathrm{sgn}(s)|s|^{\alpha}\,. \tag{13}$$

Consequently, it can be concluded that the higher-power term dominates the system, rapidly pulling its state toward the slide surface when it is far from the slide surface (with large $|s|$), and the lower-power term dominates the system, forcing its state to smoothly enter the slide mode when it approaches the slide surface (with small $|s|$).

Theorem 1 *For the slide surface switching function $s_i = e_i$ $(i = 1, 2, 3, 4)$, the error system (6) is fixed-time stable under the following control input:*

$$\begin{cases} u_1 = -\gamma_1 e_1 - k_1 \operatorname{sgn}(e_1)|e_1|^\alpha - k_2 \operatorname{sgn}(e_1)|e_1|^\beta - k_3 \operatorname{sgn}(e_1) \\ \qquad - [-ae_1 + b(M(w_1)y_1 - M(w)y) - c(y_1 z_1 - yz)] \\ u_2 = -\gamma_2 e_2 - k_1 \operatorname{sgn}(e_2)|e_2|^\alpha - k_2 \operatorname{sgn}(e_2)|e_2|^\beta - k_3 \operatorname{sgn}(e_2) - e_1 \\ u_3 = -\gamma_3 e_3 - k_1 \operatorname{sgn}(e_3)|e_3|^\alpha - k_2 \operatorname{sgn}(e_3)|e_3|^\beta - k_3 \operatorname{sgn}(e_3) - d\left(y_1^2 - y^2\right) \\ u_4 = -\gamma_4 e_4 - k_1 \operatorname{sgn}(e_4)|e_4|^\alpha - k_2 \operatorname{sgn}(e_4)|e_4|^\beta - k_3 \operatorname{sgn}(e_4) - e_2 + ke_4 \end{cases} \tag{14}$$

with $\gamma_i > 0$, k_1, k_2, $k_3 > 0$, $0 < \alpha < 1$, $\beta > 1$. That is, the drive system (2) and response system (5) achieve FxTS, and the settling time T is bounded by

$$T \leq \frac{2^{\frac{1-\alpha}{2}}}{k_1(1-\alpha)} + \frac{2^{\frac{\beta-1}{2}}}{k_2(\beta-1)}\,. \tag{15}$$

Proof. Consider the following Lyapunov function:

$$V = \frac{1}{2}\sum_{i=1}^{4} s_i^2 = \frac{1}{2}\sum_{i=1}^{4} e_i^2\,, \tag{16}$$

then the time derivative of V along the trajectories of the error system (6) can be calculated as

$$\dot{V} = \sum_{i=1}^{4} e_i \dot{e}_i = e_1\dot{e}_1 + e_2\dot{e}_2 + e_3\dot{e}_3 + e_4\dot{e}_4\,. \tag{17}$$

Substituting the error system (6) and the control input (14) into Eq. (17) and cancelling some nonlinear terms, we have

$$\begin{aligned} \dot{V} &= e_1[-\gamma_1 e_1 - k_1 \operatorname{sgn}(e_1)|e_1|^\alpha - k_2 \operatorname{sgn}(e_1)|e_1|^\beta - k_3 \operatorname{sgn}(e_1)] \\ &\quad + e_2[-\gamma_2 e_2 - k_1 \operatorname{sgn}(e_2)|e_2|^\alpha - k_2 \operatorname{sgn}(e_2)|e_2|^\beta - k_3 \operatorname{sgn}(e_2)] \\ &\quad + e_3[-\gamma_3 e_3 - k_1 \operatorname{sgn}(e_3)|e_3|^\alpha - k_2 \operatorname{sgn}(e_3)|e_3|^\beta - k_3 \operatorname{sgn}(e_3)] \\ &\quad + e_4[-\gamma_4 e_4 - k_1 \operatorname{sgn}(e_4)|e_4|^\alpha - k_2 \operatorname{sgn}(e_4)|e_4|^\beta - k_3 \operatorname{sgn}(e_4)] \\ &= -\sum_{i=1}^{4} \gamma_i e_i^2 - k_1 \sum_{i=1}^{4} |e_i|^{\alpha+1} - k_2 \sum_{i=1}^{4} |e_i|^{\beta+1} - k_3 \sum_{i=1}^{4} |e_i|\,. \end{aligned} \tag{18}$$

Since $\gamma_i > 0, k_3 > 0$, it follows that:

$$\dot{V} \leq -k_1 \sum_{i=1}^{4} |e_i|^{\alpha+1} - k_2 \sum_{i=1}^{4} |e_i|^{\beta+1}\,. \tag{19}$$

From Lemma 1, we have

$$\sum_{i=1}^{4} |e_i|^{\alpha+1} \geq \left(\sum_{i=1}^{4} e_i^2\right)^{\frac{\alpha+1}{2}}, \qquad \sum_{i=1}^{4} |e_i|^{\beta+1} \geq 4^{\frac{1-\beta}{2}} \left(\sum_{i=1}^{4} e_i^2\right)^{\frac{\beta+1}{2}}. \tag{20}$$

Thus, Eq. (19) can be written as

$$\dot{V} \leq -k_1(2V)^{\frac{\alpha+1}{2}} - k_2 4^{\frac{1-\beta}{2}} (2V)^{\frac{\beta+1}{2}}. \tag{21}$$

According to Lemma 2, we can concluded that the error system (6) is fixed-time stable, thus system (2) and system (5) achieve FxTS. The settling time T can be estimated as

$$T \leq \frac{2^{\frac{1-\alpha}{2}}}{k_1(1-\alpha)} + \frac{2^{\frac{\beta-1}{2}}}{k_2(\beta-1)}. \tag{22}$$

To directly demonstrate the effectiveness of the FxTS, we provide the simulation according to Theorem 1. Let $a = 6$, $b = c = d = 1$, and $k = 9$, then system (2) is chaotic with its strange attractor shown in Fig. 1. Let $\alpha = 0.5$ and $\beta = 1.5$ to satisfy the condition $0 < \alpha < 1 < \beta$ in Theorem 1 and let the control parameters be $k_1 = 2$, $k_2 = 1$, $k_3 = 0.2$ and $\gamma_1 = \gamma_2 = \gamma_3 = \gamma_4 = 0.5$. The initial values of system (2) and system (5) are respectively given as $X_0 = (x(0), y(0), z(0), w(0)) = (2.0, -1.0, 1.0, 0.5)$ and $Y_0 = (x_1(0), y_1(0), z_1(0), w_1(0)) = (-1.5, 1.2, 1.8, -0.6)$. Using the control input (14) in Theorem 1, we can simulate the time evolution of errors $e_1(t), e_2(t), e_3(t), e_4(t)$ as shown in Fig. 9 (a). It can be seen that the errors $e_1(t), e_2(t), e_3(t)$, and $e_4(t)$ rapidly decrease and converge to zero within a finite time regardless of the initial error values. Based on Theorem 1, the upper bound of the settling time can be calculated as $T \leq 2^{\frac{1-\alpha}{2}}/k_1(1-\alpha) + 2^{\frac{\beta-1}{2}}/k_2(\beta-1) \approx 1.1120$ s. Keeping the initial value of drive system (2) unchanged and resetting initial value of response system (5) as $Y_{01} = (-3.5, -1.2, 0.8, -0.6)$, we further illustrate the effectiveness and robustness of the proposed FxTS control method. As shown in Fig. 9 (b), the errors $e_1(t)$, $e_2(t)$, $e_3(t)$, and $e_4(t)$ rapidly approach zero within a fixed time. Moreover, the approach process is smooth without large oscillations, and the convergence times for the initial values Y_0 and Y_{01} are almost the same, which illustrates that system (2) and system (5) can realize FxTS under the designed controller, with the convergence times not affected by the initial values.

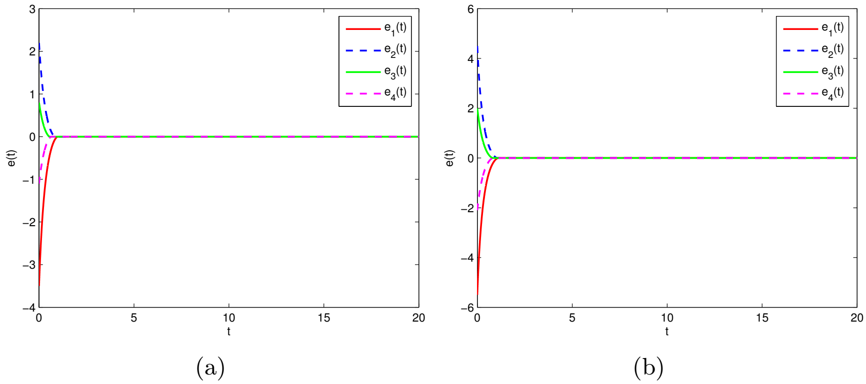

Fig. 9. The time evolution of the errors between system (2) and system (5) under different initial values: (a) Y_0; (b) Y_{01}.

5. Conclusions

This paper proposed a new MCS with an exponential term, a constant term, and only one equilibrium by coupling a memristor with an absolute-value function. The complex dynamics and FxTS of the proposed MCS were theoretically and numerically investigated. It was shown that the MCS exhibited stable, periodic, and chaotic states via Hopf bifurcation and period-doubling bifurcation as the parameters vary. The boundaries of the chaotic attractors and the oscillation amplitudes of the variables undergo large-scale expansion as the parameter values continuously increase, implying the existence of large-scale amplitude modulation in the system. Furthermore, the FxTS problem was discussed, and the corresponding FxTS conditions were obtained by applying a slide mode controller with the designed power reaching law via theoretical derivation and simulation analysis. The discovery of the memristor has revealed many uncertain and mysterious effects in chaotic systems which has inspired increasing attention to MCS. More and more in-depth achievements on MCS are expected in future work.

REFERENCES

[1] E.N. Lorenz, «Deterministic Nonperiodic Flow», *J. Atmos. Sci.* **20**, 130 (1963).

[2] G. Chen, D. Lai, «Making a dynamical system chaotic: feedback control of Lyapunov exponents for discrete-time dynamical systems», *IEEE Trans. Circuits Syst. I* **44**, 250 (1997).

[3] J.C. Sprott, «Elegant Chaos: Algebraically Simple Chaotic Flows», *World Scientific*, 2010.

[4] L. Chua, «Memristor — The missing circuit element», *IEEE Trans. Circuit Theory* **18**, 507 (1971).

[5] D.B. Strukov, G.S. Snider, D.R. Stewart, R.S. Williams, «The missing memristor found», *Nature* **453**, 80 (2008).

[6] Q. Lai, M. Qin, «Universal Method for Enhancing Dynamics in Neural Networks via Memristor and Application in IoT-Based Robot Navigation», *IEEE Trans. Cybern.* **56**, 557 (2026).

[7] Q. Lai, J. Wang, «Diverse dynamical behaviors and predefined-time synchronization of a simple memristive chaotic system», *Acta Phys. Sinica* **74**, 200501 (2025).

[8] Q. Lai, H. Hua, L. Yang, «Encryption Design and Analysis of 3-D Medical Models in Internet of Medical Things Using a Novel Memristive Hyperchaotic Map», *IEEE Internet Things J.* **12**, 39019 (2025).

[9] J. Zhang *et al.*, «Design, analysis and application of Non-Hamiltonian conservative chaotic system based on memristor», *Integration* **100**, 102307 (2025).

[10] Y. Diao *et al.*, «Generating any number of multi-butterfly chaotic attractors via a novel memristor with only one internal function», *Chaos Solit. Fract.* **188**, 115526 (2024).

[11] B. Zhang, N. Zhou, S. Zhou, M. Wang, «Novel 4D chaotic system based on memristor and its application in secure color image encryption», *Digit. Signal Process.* **170**, 105791 (2026).

[12] O.M. Njimah *et al.*, «Coexisting oscillations and four-scroll chaotic attractors in a pair of coupled memristor-based Duffing oscillators: Theoretical analysis and circuit simulation», *Chaos Solit. Fract.* **166**, 112983 (2023).

[13] H. Chang, B. Han, Y. Zhang, Y. Li, «A novel memristive chaotic system with ubiquitous extreme multistability», *Chaos Solit. Fract.* **203**, 117599 (2026).

[14] B. Xu, X. Ye, «A Memtransistor–Memristor-Based Chaotic Circuit with Attractors Coexistence», *Mathematics* **14**, 2027 (2026).

[15] X. Zhang, Q. Liu, «Memristor chaos: A Jacobi instability perspective», *Phys. Lett. A* **580**, 131531 (2026).

[16] S. Shi, L. Liu, C. Du, Z. Zhang, «Analysis of the complexity and dynamical characteristics of chaotic systems under different memristor models», *Phys. Scr.* **101**, 035203 (2026).

[17] H. Li, F. Min, J. Ying, «A nonvolatile multistable discrete locally active memristor and its switching dynamics», *Chaos Solit. Fract.* **206**, 117897 (2026).

[18] Q. Wu *et al.*, «Discrete Exponential Memristor-Coupled Multistable Hyperchaotic Attractor», *Mathematics* **14**, 1648 (2026).

[19] S. Rajagopal *et al.*, «Locally active memristor-based Chialvo neuron model: bifurcation, multistability, and noise effects», *Cogn. Neurodyn.* **20**, 99 (2026).

[20] D.R. Chialvo, «Generic excitable dynamics on a two-dimensional map», *Chaos Solit. Fract.* **5**, 461 (1995).

[21] J.L. Randrianantenaina, A.Y. Baran, N. Korkmaz, R. Kilic, «Design and FPAA simulation of multi-scroll attractors in a memristor-based Hopfield neural network», *Chaos Solit. Fract.* **201**, 117386 (2025).

[22] L. Ryashko, I. Bashkirtseva, «How a memristor enhances the stochastic excitability of a map-based neuron model», *Chaos Solit. Fract.* **208**, 118236 (2026).

[23] L. Wang, T. Dong, M. Ge, «Finite-time synchronization of memristor chaotic systems and its application in image encryption», *Appl. Math. Comput.* **347**, 293 (2019).

[24] Q. Lu, Y. Feng, «A fixed-time sliding mode control scheme for synchronizing memristor-based four-dimensional hyperchaotic systems», *Phys. Scr.* **101**, 205214 (2026).

[25] J. Luo, S. Qu, Y. Chen, Z. Xiong, «Synchronization of memristor-based chaotic systems by a simplified control and its application to image en-/decryption using DNA encoding», *Chin. J. Phys.* **62**, 374 (2019).

[26] Q. Lai *et al.*, «Dynamic analysis and synchronization control of an unusual chaotic system with exponential term and coexisting attractors», *Chin. J. Phys.* **56**, 2837 (2018).